AT39.3/117

Mm performance of the ATCA antennas III: compensating for the effects of gravity deformation

Ravi Subrahmanyan
Sep 2002

Based on the VMS survey of the compact array antenna CA02, the effects of gravity deformation were examined in AT 39.3/115. The dominant cause of gain loss and beam distortion was identified to be the deformation of the main reflector surface with elevation. This report examines whether active displacements in the sub-reflector and/or feed might compensate for the aperture wavefront errors. All computations are for operation at 90 GHz.

The aperture phase errors

The gravity displacements of the feed and sub-reflector were evaluated in AT39.3/115 to be within ±1 mm. The deformation of the main reflector corresponded to surface displacements, normal to the surface, within ±1.5 mm and the r.m.s. displacement was a maximum of 0.5 mm at a declination of 15 degrees. The antenna beam patterns and gain loss at elevations of 15, 30, 45, 60, 75 and 90 degrees, for the gravity-deformed ATCA antenna, were computed in that report using ray-tracing (GO; geometric optics approximation).

The mm displacements in the optics are very much smaller than the dimensions of the antenna and the propagation path lengths between the optics components; therefore, we would expect that the change in the amplitude of the aperture illumination would be insignificant. The gain loss and distortions to the beam patterns are almost completely a consequence of aperture phase distortions.

The beam patterns computed for the gravity deformed ATCA antenna in AT39.3/115 are reproduced in Fig. 1 for reference. I have transformed these beam patterns to derive the complex aperture voltage distributions. The aperture phase distributions are shown in Fig. 2; it is assumed that the optics have been aligned at 60 degrees elevation and, therefore, the aperture phase is flat at that elevation. Linear phase gradients across the aperture, which correspond simply to a pointing shift, have been subtracted. A constant phase, corresponding to the phase of the vector sum of the aperture field distribution, has also been subtracted from all the phase distribution images. The phase variation across the aperture that is shown in Fig. 2 is the cause of the gain loss and beam pattern distortions. The aim of this report is to explore ways by which axial and off-axis displacements in the SR and feed may reduce the phase variations and, thereby, improve the gain loss and the beam patterns.

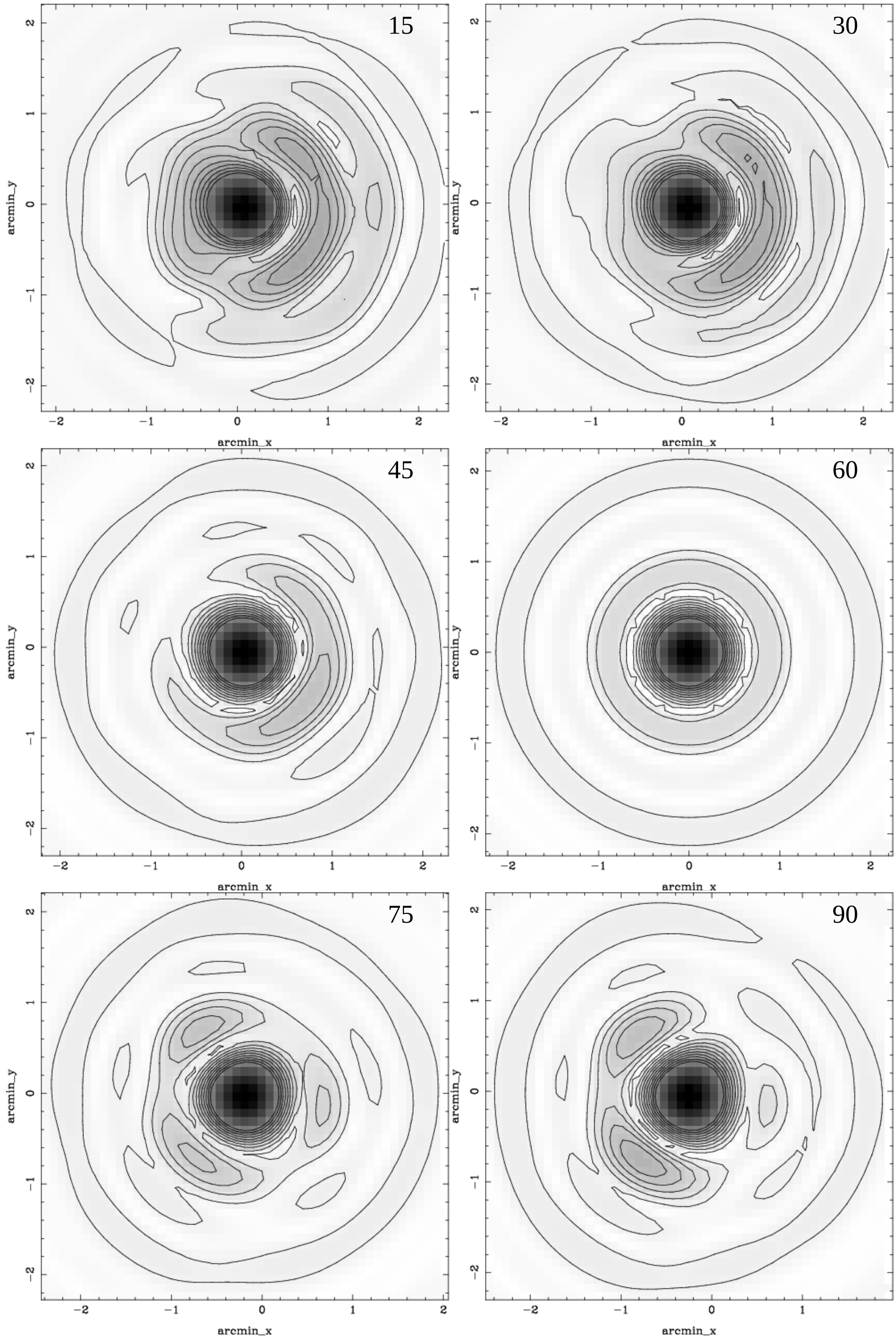

Figure 1: The 90 GHz beam patterns computed for the different elevations assuming gravity deformations as measured by the photogrammetry survey. The amplitude of the voltage pattern is shown. Contours are at 5% intervals; the maximum contour is at 50% of the peak. North is to the left of the panels.

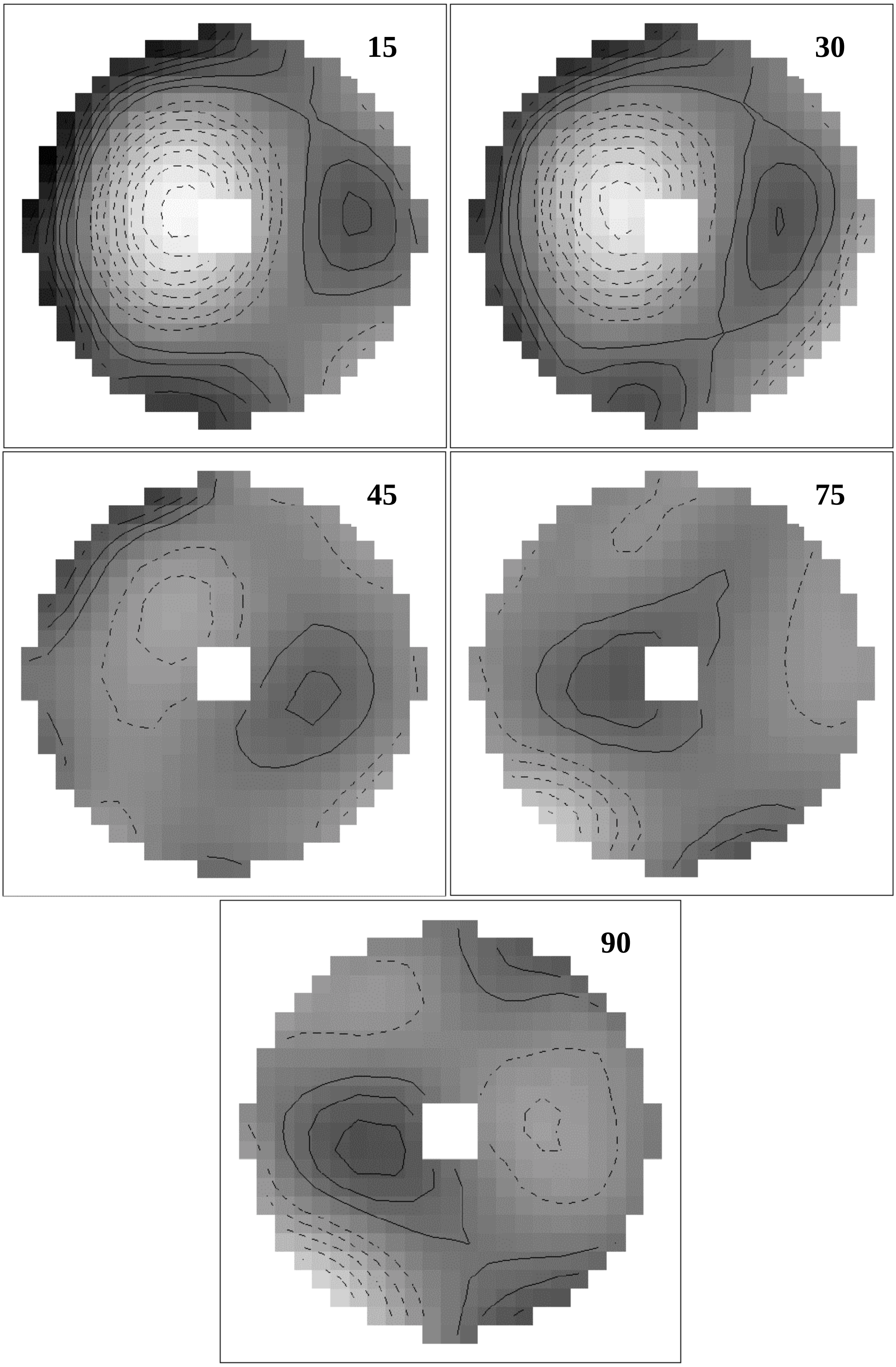

Figure 2: Aperture phase distributions computed for the gravity deformed ATCA antenna. Grey-scale spans the range ±90 degrees; contours are at 10 deg. intervals with the 0 deg. contour omitted.

Axial focus adjustment

The effects of tilts and displacements in the SR and feed are analysed in AT39.3/113. The aperture phase distribution resulting from SR tilts, or off-axis displacements of the feed or SR, are shown in the figures of that document. The phase error patterns arising from these off-axis displacements are very similar in form and are anti-symmetric about a line through the centre of the aperture. On the other hand, axial displacements of the feed or SR result in axially symmetric, or radial, phase errors.

As a first step, I have isolated the radial part of the aperture phase variations that are displayed in Fig. 2. I show the radial phase variations in Fig. 3 versus the distance from the centre of the antenna aperture; the phase at any distance from the centre of the aperture has been computed as an average in a circular ring. This radial phase may be removed, to first order, by an axial focus adjustment.

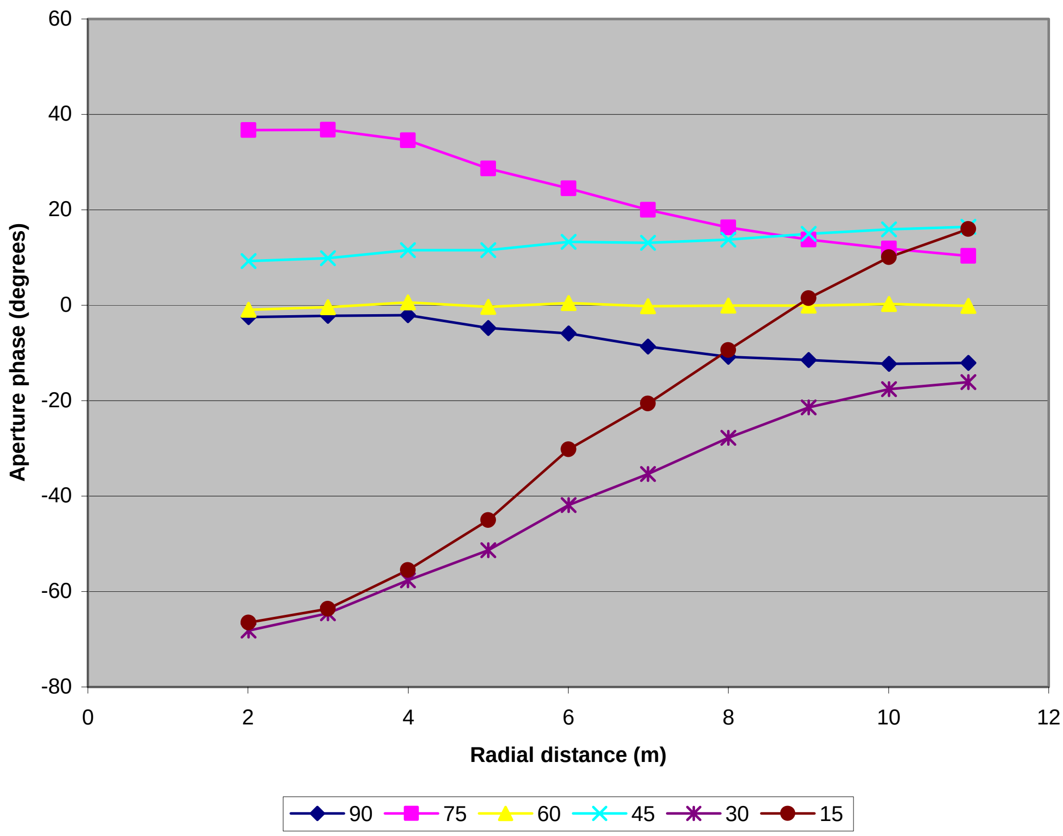

Figure 3: Aperture phase versus radius. The phase has been averaged in rings about the centre of the aperture.

In practice, the simplest axial optics adjustment that we may make is an axial displacement of the SR. At each of the survey elevations, I have iteratively converged on a value for the SR axial displacement that would yield the best improvement in the antenna gain. The optimal SR movement, at each of the survey elevations, has been computed to within ±0.05 mm. Accuracy in the SR focus adjustment of this magnitude is sufficient to keep the residual error to well within half a percent. These computed displacements are listed in Table 1 along with the expectations for the antenna gain before and after the axial adjustment.

Elevation (degrees)	Antenna gain before displacement	SR axial offset (mm)	Antenna gain after displacement
15	69	–1.2	86
30	77	–0.8	85
45	95	–0.1	95
75	94	+0.4	97
90	93	+0.2	93

Table 1: The improvement in antenna power gain with axial focus. The antenna power gains are given in columns 2 & 4 as percentages of the value expected for aligned optics.

As expected, the radial phase variation is smallest in those cases where the aperture phase distribution is anti-symmetric. And the optimal SR axial displacement is small in those cases where the radial phase variation is small. And in those cases the improvement in gain is also small. At elevation of 45 degrees, the aperture phase appears almost entirely anti-symmetric and no significant gain improvement is expected with an axial focus adjustment. At the other extreme, the radial phase change is the greatest when the antenna elevation is 15 degrees: here the gravity deformation has changed the antenna focus by as much as 1.2 mm and a repositioning of the SR by this amount recovers 17% of the gain loss.

With these axial SR focus adjustments, the computed aperture phase distributions and the corresponding beam patterns are shown in Figs. 4 & 5. The asymmetry in the beam patterns is unchanged; the coma lobes are not diminished and this is to be expected because the beam pattern asymmetries arise from the anti-symmetric part of the aperture phase error. The improvement is in the depth of the nulls of the beam patterns. With the axial focus adjustments, the aperture phase variations shown in Fig. 4 are now anti-symmetric functions; most of the radial phase variations have been removed.

The lack of a significant change in the side-lobe heights should not be taken to imply that the mosaicing performance of the array would not improve with simple axial SR adjustments. The limitations posed by antenna beam asymmetries to mosaic imaging of extended emission may be viewed as arising from visibility domain phase errors owing to aperture plane phase variations. The significant reduction in the aperture phase variations, as seen in comparing Fig. 4 with Fig. 2, may be expected to result in an improvement in the visibility domain phase errors and, consequently, will improve the mosaic imaging capability of the array.

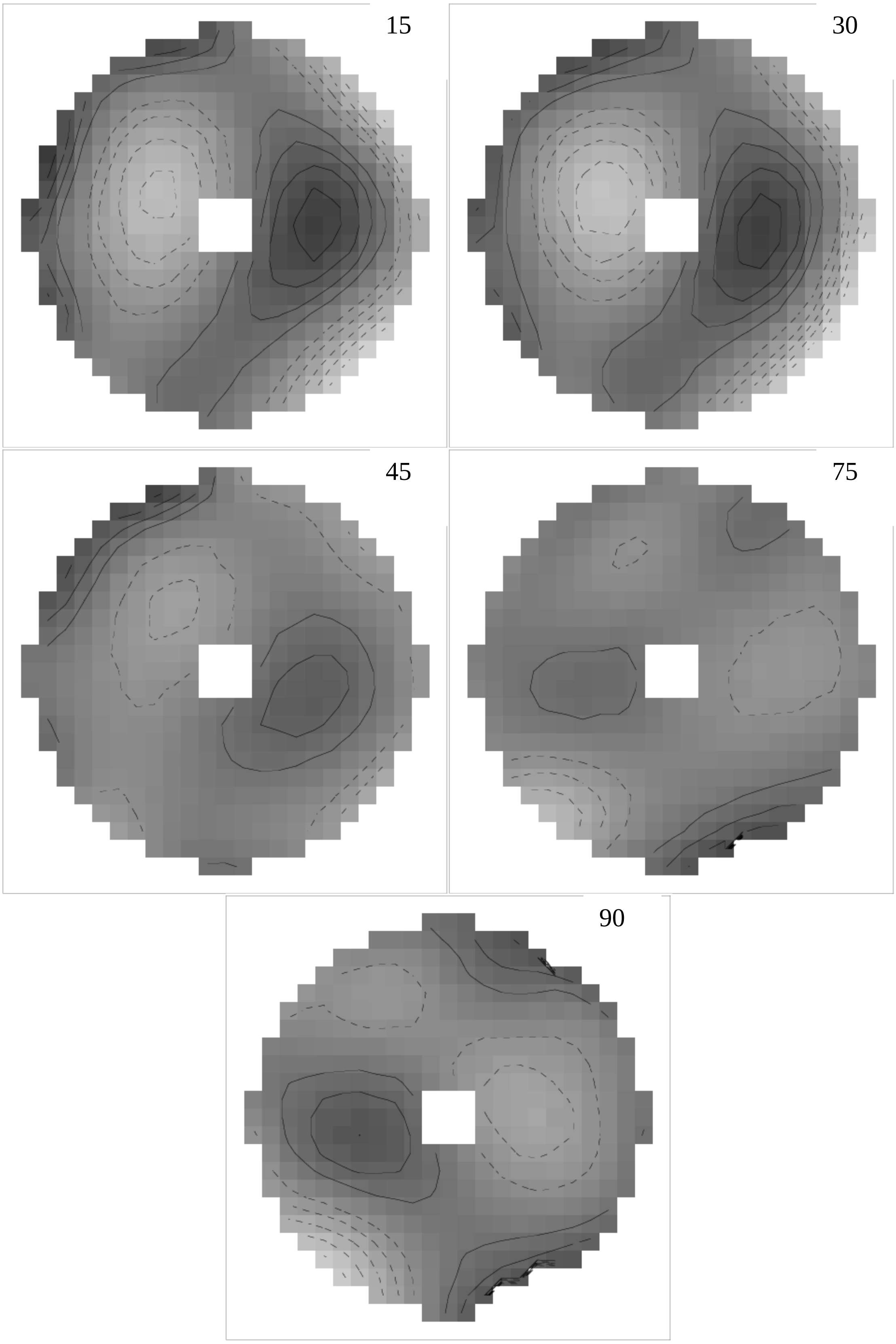

Figure 4: Aperture phase distributions for the gravity deformed antenna with optimal SR axial movement to compensate for the gain loss. Grey-scale spans the range ±90 degrees; contours are at 10 deg. intervals with the 0 deg. contour omitted.

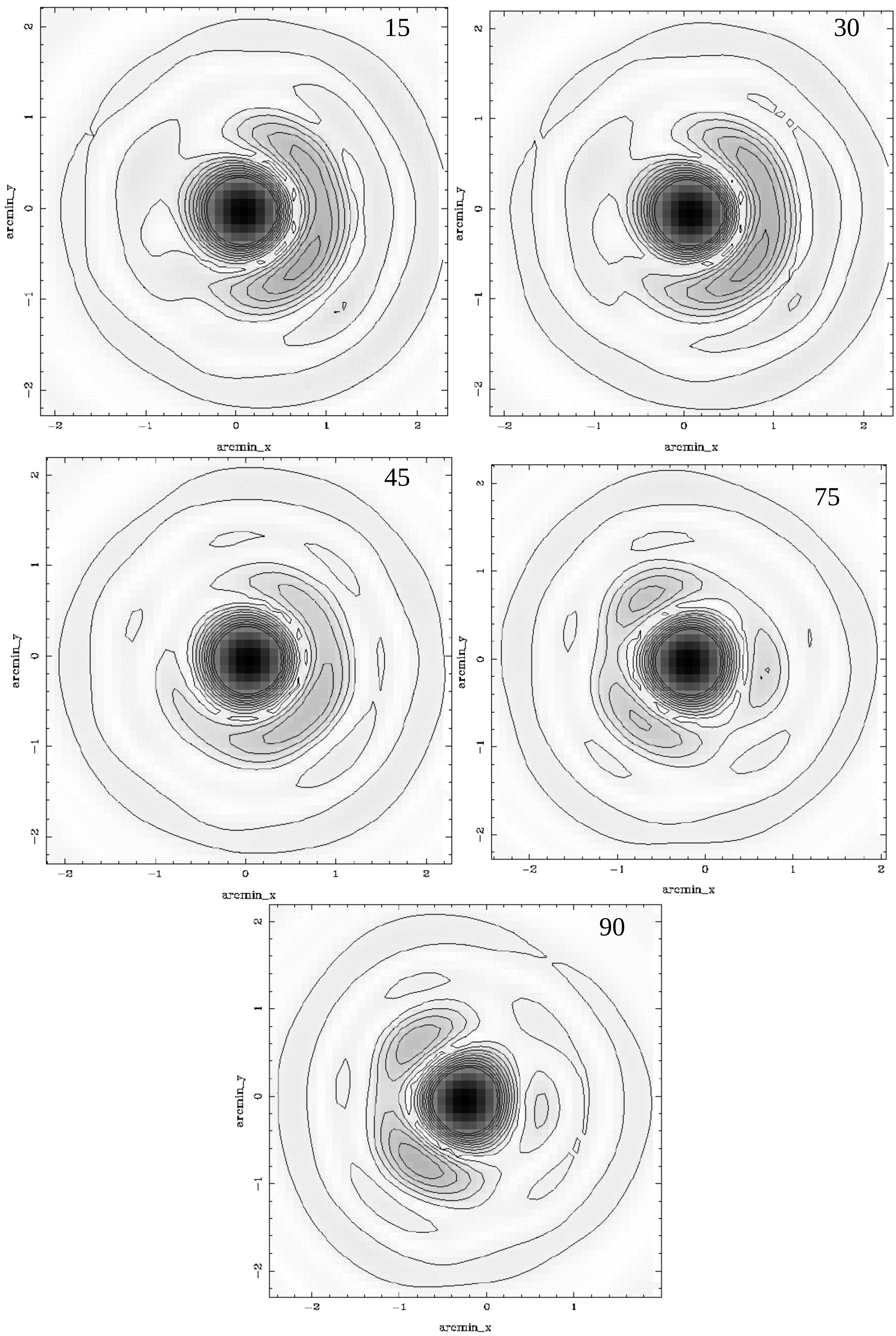

Figure 5: The beam patterns computed for the different elevations with gravity deformations compensated for with optimal SR axial displacement. The amplitude of the voltage pattern is shown. Contours are at 5% intervals; the maximum contour is at 50% of the peak. North is to the left of the panels.

An axial SR displacement +
an off-axis feed displacement perpendicular to the elevation axis

The next step is an off-axis displacement to remove the anti-symmetric part of the aperture phase error. The off-axis adjustment could, in principle, be implemented as either one of (i) a lateral feed offset, (ii) a lateral SR displacement, or (iii) a tilt to the SR; either of these would give an anti-symmetric aperture phase that could compensate for the anti-symmetric part of the phase error produced by the gravity deformation. Multiple off-axis movements may make higher order corrections to the aperture phase: because the form of the aperture phase produced by SR rotations are very nearly that produced by feed offsets (this is shown in AT39.3/113), I would recommend combining SR displacements with either one of SR rotations or feed displacements as a useful pair of movements. In this report I shall only consider first order corrections.

I continue to adopt the right-handed x, y, z Cartesian coordinate frame shown in Fig. 1 of AT39.3/115. To repeat here the convention that is adopted, the z axis is along the optical axis of the antenna, the x axis is on the aperture plane and directed opposite to the lightning rod, the y axis is again on the aperture plane and parallel to the elevation axis. With the antenna tipped in elevation, N is up the aperture plane and towards the lightning rod (towards negative x) and E is towards positive y. Rotations about any axis follow the convention for a right-handed screw. A pair of components along the x and y-axes describes the off-axis displacement vectors whereas a pair of rotations about the x and y-axes describes tilts in the SR.

I have first examined the improvement in gain loss, at each of the survey elevations, with lateral displacements in the feed. This lateral displacement is in addition to the axial SR displacement discussed in the previous section. Additionally, in this section I restrict the feed displacement to be along the x-axis, which is in the aperture plane and perpendicular to the elevation axis. Because gravity acts in the x-z plane, we expect the dominant anti-symmetric phase errors to be the component anti-symmetric about the y-axis, and this ought to be removed, to first order, with an x-axis displacement of the feed.

The computed optimal SR axial displacement, and optimal x-axis feed displacement, which best compensate for the gain loss, are listed in Table 2 for the different elevations. The feed offsets have been determined to within ±0.5 mm. The relative antenna power gains, before and after these displacements, are also listed in the table. The improvement in antenna gain is remarkable. The GO analysis shows that the axial focus along with 1D feed translation perpendicular to the elevation axis may recover most of the gain loss and the residual aperture phase errors will result in a maximum gain loss of 4%.

Elevation (degrees)	Antenna gain before displacement	SR axial offset (mm)	Feed offset along x (mm)	Antenna gain after displacement
15	69	–1.2	+12	96
30	77	–0.8	+13	96
45	95	–0.1	+6	99
75	94	+0.4	–3	98
90	93	+0.2	–7	96

Table 2: The improvement in antenna power gain with axial focus and x-axis feed displacement. The antenna power gains are given in columns 2 & 5 as percentages of the optimal gain for aligned optics.

The residual aperture phase error distributions after these two compensating displacements are shown in Fig. 6. The vertical axis in these plots is parallel to the elevation axis. The aperture phase error is now within about ±20 degrees. The dominant anti-symmetric phase error obvious in the plots in Fig. 4 at most elevations is now absent: the off-axis displacement has successfully compensated for most of this phase error component.

The corresponding antenna beam patterns are shown in Fig. 7. As expected, the beam symmetry is considerably improved: the coma lobes are reduced and at elevation 30 degrees, they have decreased from a 10% level to a 4% level in the antenna power patterns. The higher order errors seen in the beam patterns at high elevation is not significantly altered.

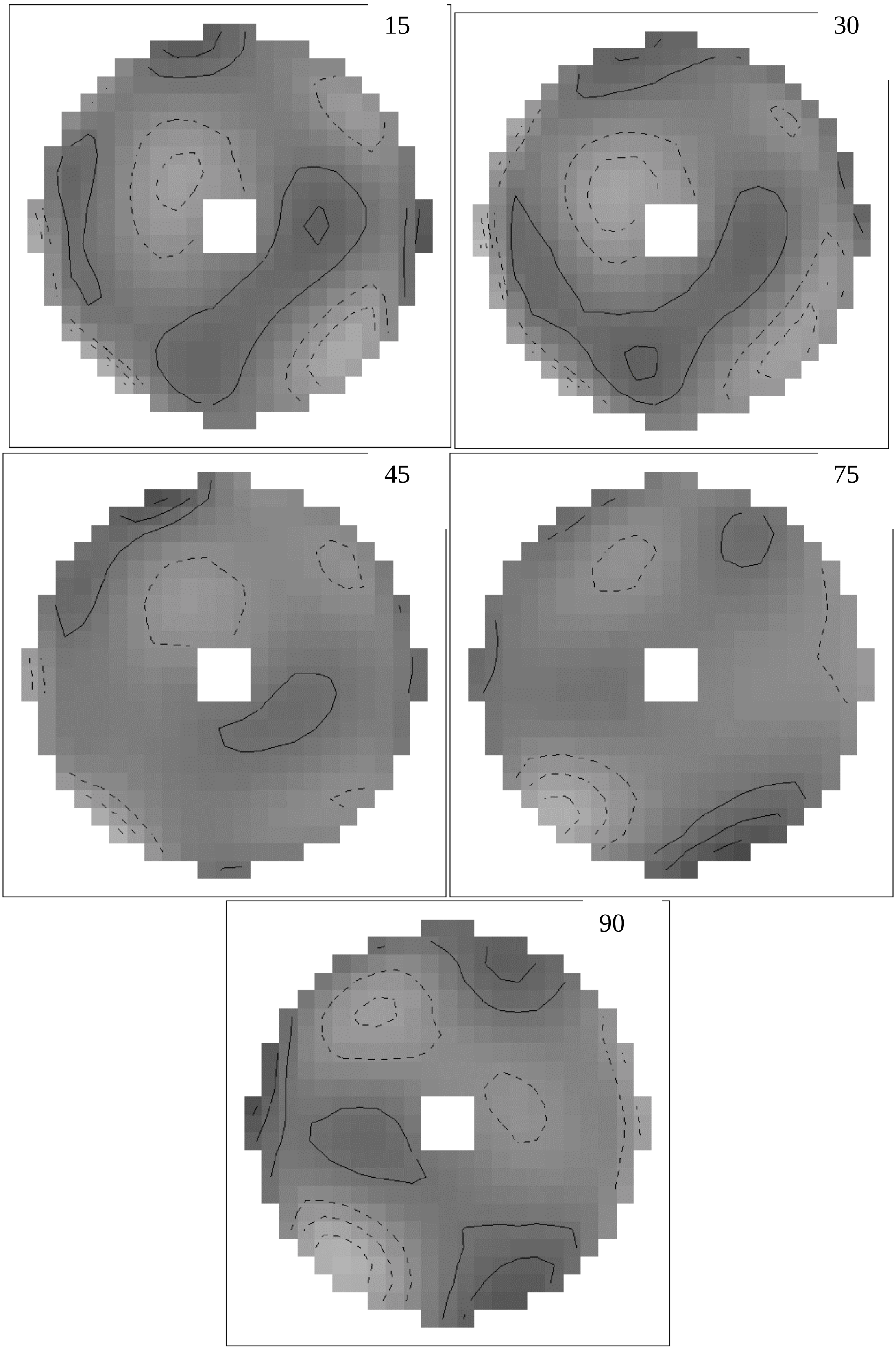

Figure 6: Aperture phase distributions for the gravity deformed antenna with optimal SR axial movement and x-axis feed displacements compensating for the gain loss. Grey-scale spans the range ±90 degrees; contours are at 10 deg. intervals with the 0 deg. contour omitted. North on the aperture plane is to the left of the figures.

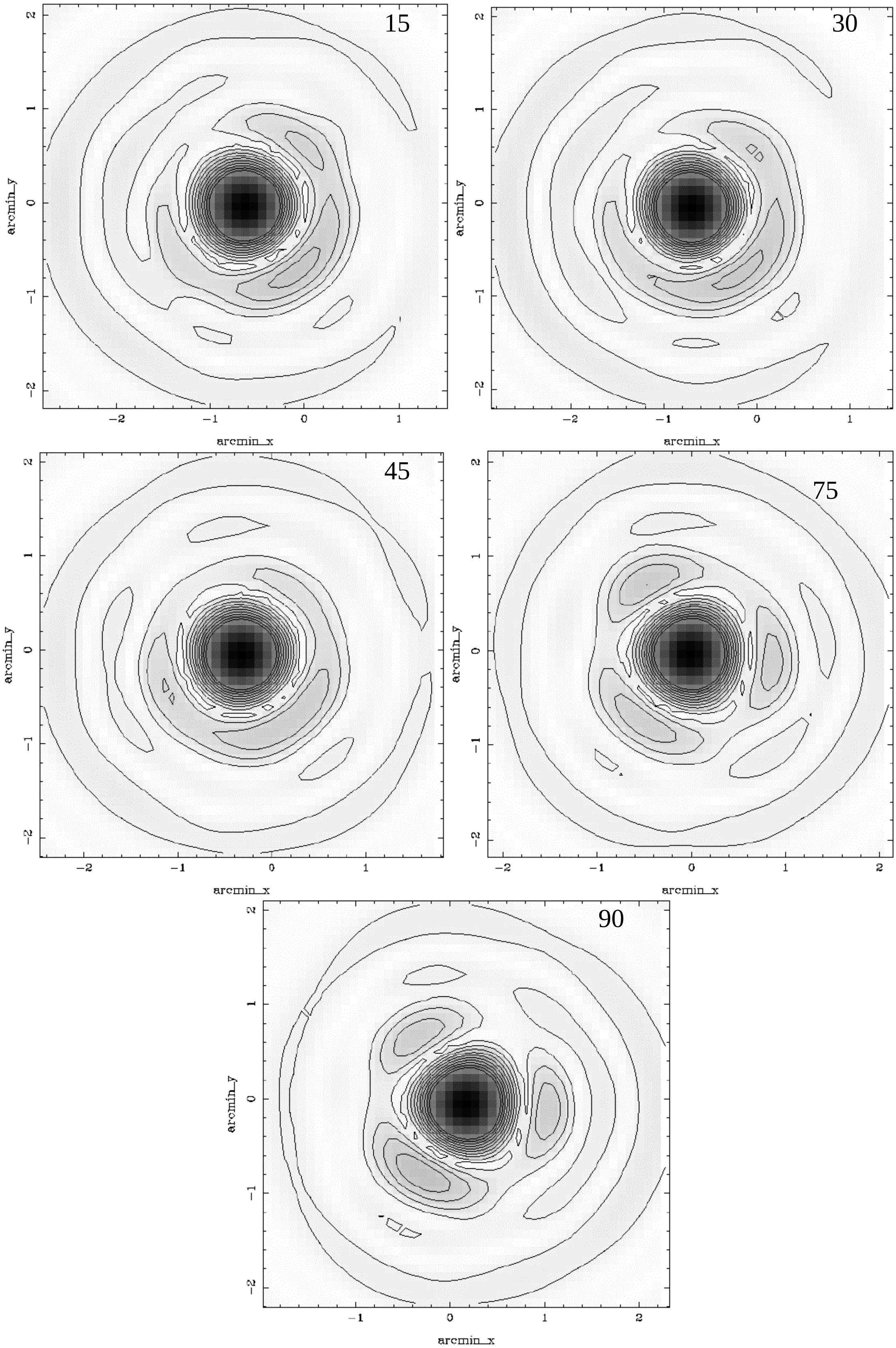

Figure 7: The beam patterns computed for the different elevations with gravity deformations compensated for with optimal SR axial displacements and feed x-axis displacements. The amplitude of the voltage pattern is shown. Contours are at 5% intervals; the maximum contour is at 50% of the peak. North is to the left of the panels.

An axial SR z displacement + x-y plane feed displacement

As a third step, I have allowed the feed a 2-component displacement in the x-y aperture plane. The optimal SR axial displacement, along with the optimal feed displacement components along the x and y-axes, are given in Table 3 for each of the survey elevations.

Elevation (degrees)	Antenna gain before displacements	SR axial offset (mm)	Feed offset along x (mm)	Feed offset along y (mm)	Antenna gain after displacements
15	69	–1.2	+12	–3	97
30	77	–0.8	+13	–4	97
45	95	–0.1	+6	–3	99
75	94	+0.4	–3	0	98
90	93	+0.2	–7	–3	97

Table 3: The improvement in antenna power gain with axial focus and x,y-plane feed displacement. The antenna power gains are given in columns 5 & 6 as percentages of the maximum possible value.

The addition of this further degree of freedom has made a marginal improvement in antenna gain. The improvement is at the 1% level. With the y-axis feed movement, the gain loss is computed to be a maximum of 3% over the entire 15-90 degree elevation range. The increase in complexity of implementing a 2-component off-axis displacement mechanism, in contrast to a single x-component displacement, has to be viewed in the light of this marginal improvement in the antenna gain.

The residual aperture phase errors after the axial z-axis SR displcement and x,y-component feed displacements is shown in Fig. 8. The corresponding antenna beam patterns are in Fig. 9. The aperture phase errors are marginally improved; the symmetry in the beam side-lobes is improved. As expected from the marginal gain improvements with y-component feed displacements, the aperture phase errors and beam quality are not significantly improved with this additional degree of freedom for the feed displacement.

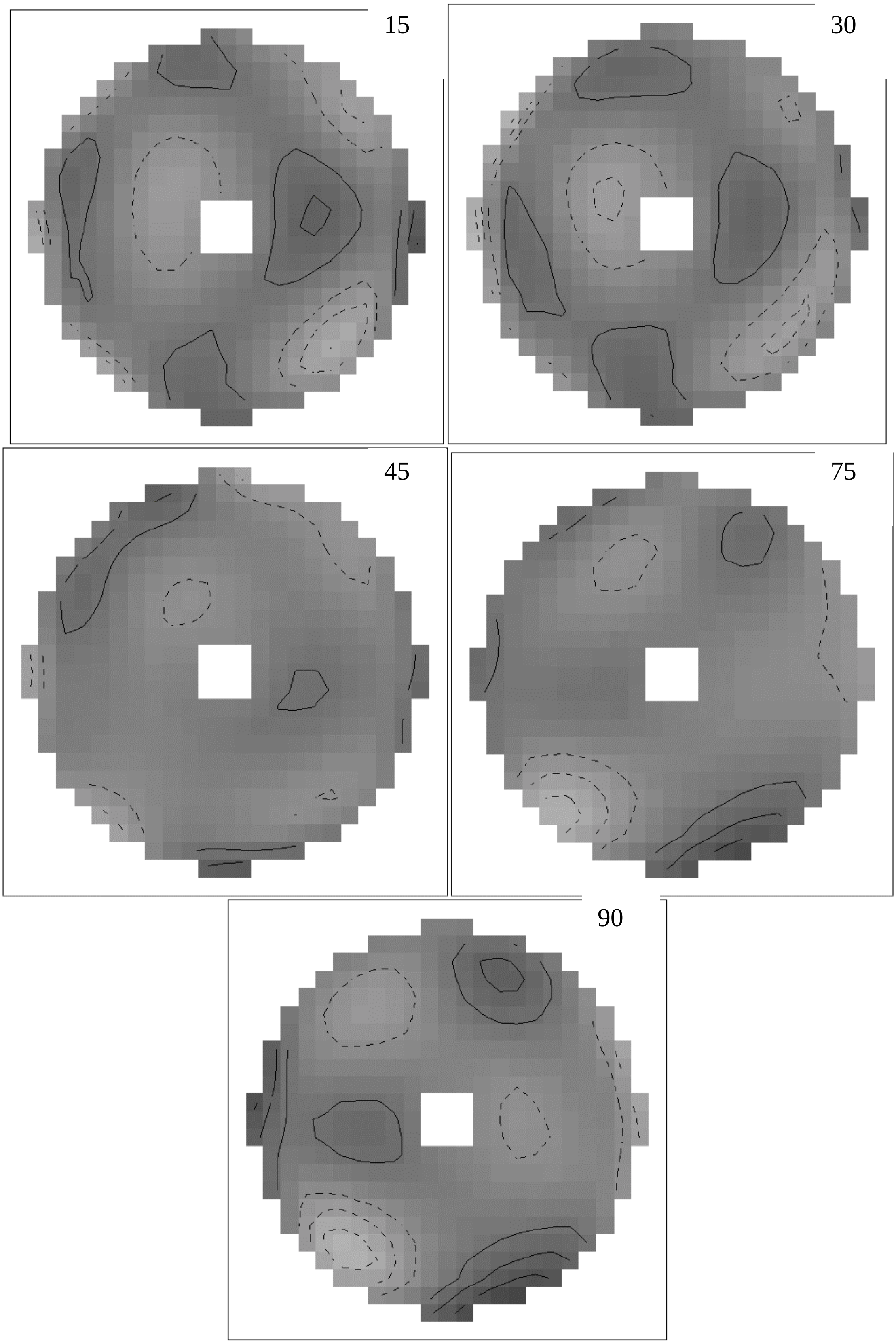

Figure 8: Aperture phase distributions for the gravity deformed antenna with optimal SR axial movement and x-y plane feed displacements compensating for the gain loss. Grey-scale spans the range ±90 degrees; contours are at 10 deg. intervals with the 0 deg. contour omitted.

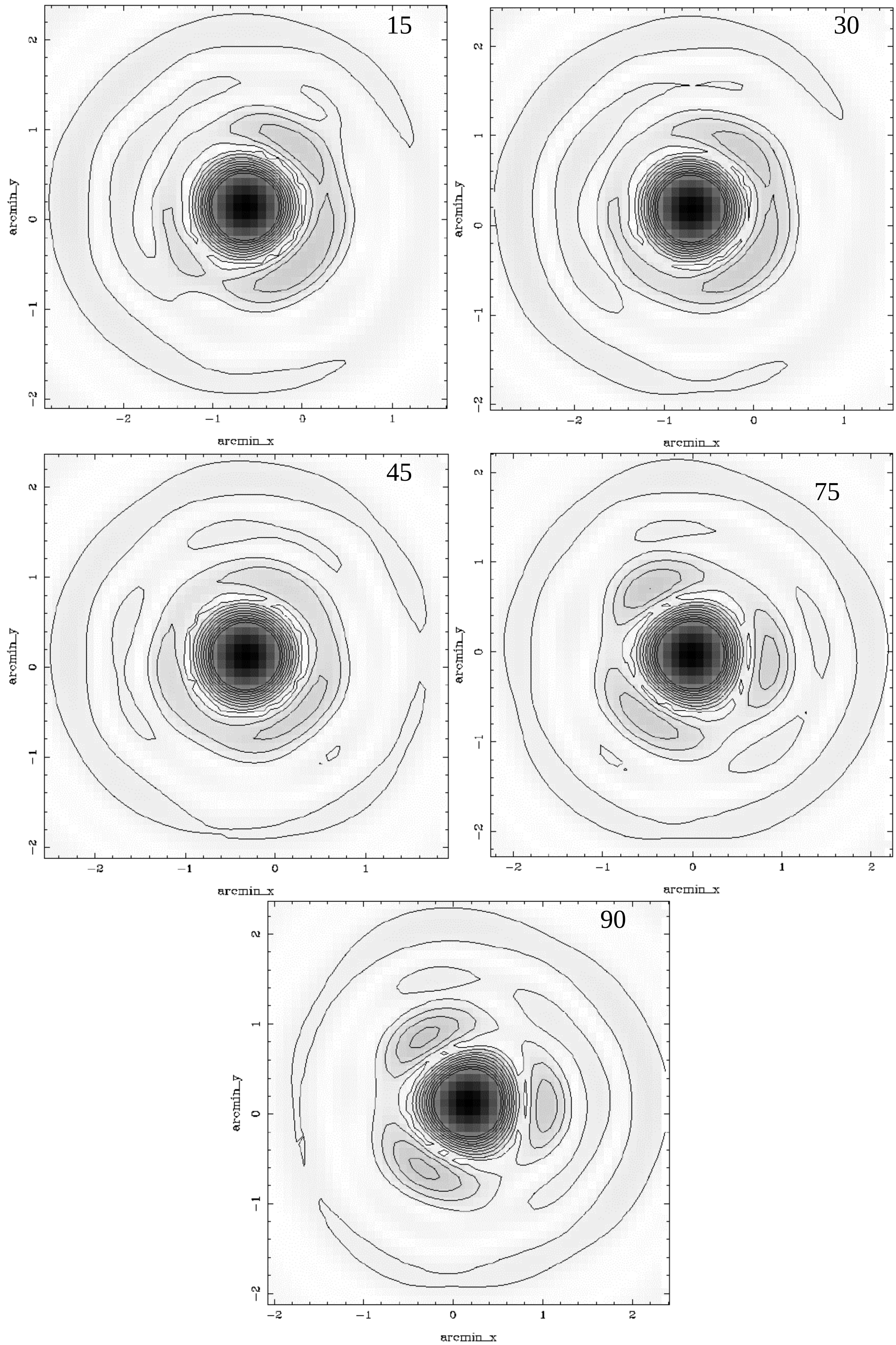

Figure 9: The beam patterns computed for the different elevations with gravity deformations compensated for with optimal SR axial displacements and feed x-y plane displacements. The amplitude of the voltage pattern is shown. Contours are at 5% intervals; the maximum contour is at 50% of the peak. North is to the left of the panels

A summary of the relative antenna gains at the different survey elevations, for the different compensating displacements, is shown in Fig. 10.

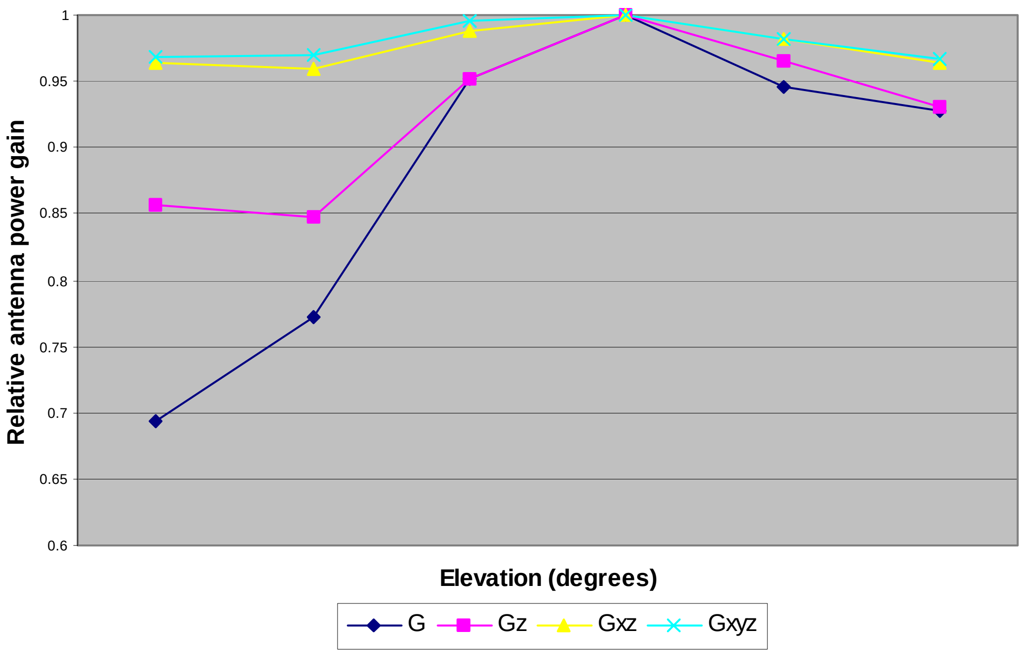

Figure 10: The antenna power gain versus survey elevation. The antenna power gains are normalized to the value at 60 degrees elevation, where the optics is assumed to be aligned and there are zero gravity deformation related misalignments. G represents gains without any compensation for gravity deformation; Gz is the gain with optimal SR z-axis displacement, Gxz is the gain with an additional x-axis feed displacement and Gxyz is for SR axial focus plus feed xy-plane adjustments.

SR axial z-axis displacement + SR lateral displacements:

In place of feed translation in the aperture plane, the anti-symmetric phase errors may be compensated with offsets to the SR in the x-y plane. For illustration, I have examined the case for the compensation at elevation 30 degrees. The feed displacements of +13 mm along x-axis and –4 mm along y-axis are replaced by SR displacements of –2.0 mm along x-axis and +0.6 mm along y-axis. As before, the SR is also displaced along z-axis by –0.8 mm to compensate for the axial focus shift.

The resulting aperture phase error and antenna beam patterns are shown in Fig. 11. The phase errors here are marginally smaller than in the case where the compensation was achieved via feed translation. The gain is now computed to be 0.98 of the optimum peak value; this is about 1.5% better than the case where the compensation was achieved by feed translation.

I have examined the relative gain improvements, at all the survey elevations, for the case where SR lateral shifts are used in place of feed lateral shifts: at low elevations, there is marginally (at the 1.5% level) better recovery of the gain loss with SR shifts, but at higher elevations, I see no difference between the two options.

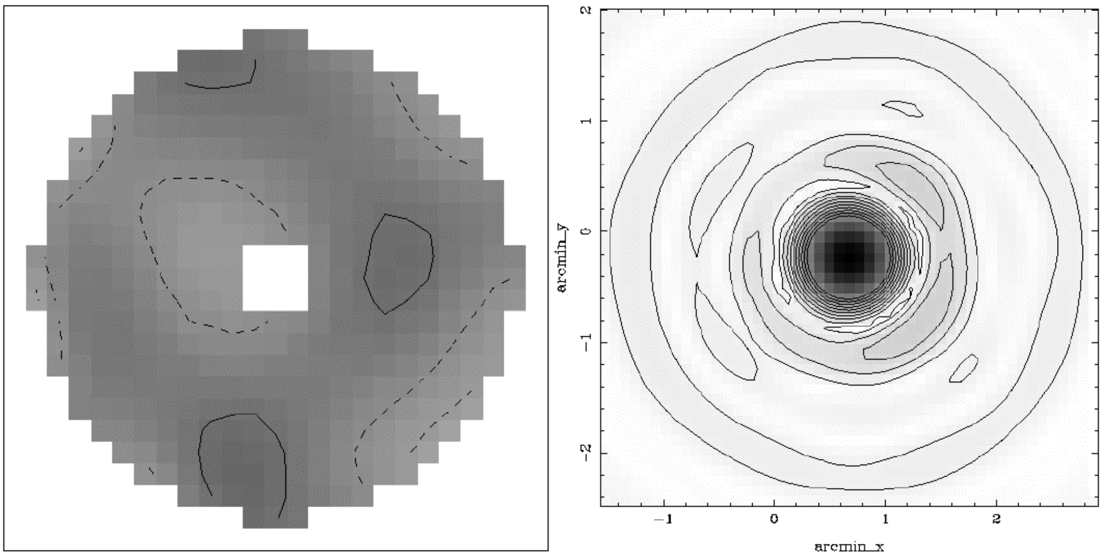

Figure 11: The aperture phase distribution and beam pattern of the AT antenna at 30 deg. elevation with the gravity deformation optimally compensated for by an SR axial displacement of $\Delta z=-0.8$ mm and SR lateral displacements of $\Delta x=-2.0$ mm and $\Delta y=+0.6$ mm. The amplitude of the voltage pattern is shown with contours at 5% intervals; the maximum contour is at 50% of the peak. For the phase plot, gray-scale spans the range ±90 degrees with contours at 10 deg. intervals and with the 0 deg. contour omitted**.** North is to the left of the panels.

SR axial z-axis displacement + SR rotations:

Another option is to compensate the anti-symmetric phase errors via SR rotations about the x and y-axes. Here again I've considered the gravity deformations at 30 degrees elevation. Instead of the +13 mm x-axis feed displacement and the –4 mm y-axis feed displacement, I've considered rotations of the SR about the x-axis by 0.02 degrees and about the y-axis by 0.065 degrees. Both the rotations are positive implying that the eastern and northern ends of the SR shift upwards and away from the main reflector. Additionally, the SR is also displaced –0.8 mm along z.

The residual aperture phase errors and antenna beam patterns are shown in Fig. 12. The differences between these distributions and the cases where the off-axis displacements were put in as SR displacements or feed displacements are marginal. The antenna power gain in this case is 96% of the optimum value; this is within 1% of what was achieved with feed displacements.

At the 1% level, the GO computation implies that SR displacements are to be preferred over SR rotations and feed displacements.

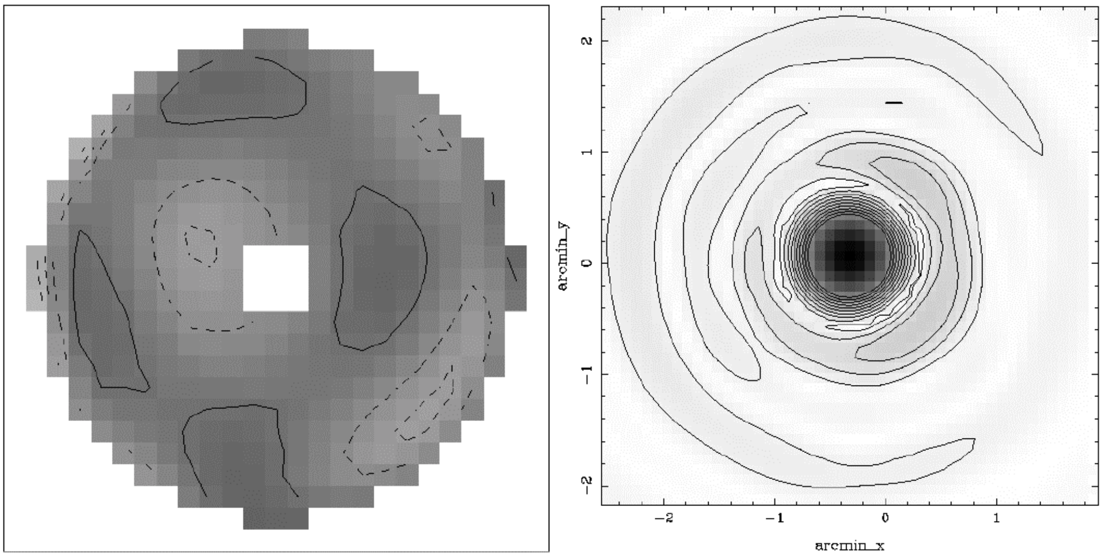

Figure 12: The beam pattern and aperture phase distributions of the AT antenna at 30 deg. elevation with the gravity deformation optimally compensated for by an SR axial displacement of Δz=–0.8 mm and SR rotations of +0.02 deg. about the x-axis and +0.065 deg. about the y-axis. The amplitude of the voltage pattern is shown with contours at 5% intervals; the maximum contour is at 50% of the peak. For the phase plot, gray-scale spans the range ±90 degrees with contours at 10 deg. intervals and with the 0 deg. contour omitted**.** North is to the left of the panels.

Antenna phase

An aspect that is of relevance is the antenna phase change with gravity deformation and the change in antenna phase as a consequence of correcting for the gain loss with displacements to the optics. In the interferometer, if all antennas deform identically and if the compensating displacements were identical, the baseline phases would be unaffected; however, differences between antennas would result in a frequency dependent phase error. In the following Table 4 I tabulate the antenna phases computed at 90 GHz for the various cases.

Antenna elevation	Phase of the gravity deformed antenna	Phase after the z-axis SR focus adjustment	Phase with z-axis SR focus and x-axis feed displacement	Phase with SR z-axis focus and feed xy displacements
15	-15	188	186	186
30	-33	101	100	99
45	14	30	30	30
75	19	-49	-49	-49
90	-9	-42	-43	-43

Table 4: The antenna phase at 90 GHz.

The axial SR focus adjustment significantly changes the antenna phase at 90 GHz. If the focus were altered actively during interferometric observations in the 3 mm band, and if the adjustments were not exactly the same in all antennas, the visibility phases would require an antenna-based correction. The off-axis displacements do not change the antenna phase; these might be actively altered without any change to the antenna phase.

A curious aspect brought out by Table 4 is that gravity deformations, by themselves, cause only a phase change of about 50 degrees over the entire elevation range 15-90 degrees. The gravity induced defocusing does not change the phase as much as the re-focussing via SR axial movement.

Antenna pointing

Another aspect that would have to be addressed if any off-axis displacements were made to the antenna optics components is the resultant shift in the antenna pointing. Active off-axis displacements would need to be accompanied by an updating of the antenna pointing parameters.

Imaging dynamic range

An r.m.s. phase error of $\Delta\varphi$ degrees on the aperture would result in an antenna power gain loss factor of $\cos^2(\Delta\varphi)$. In mosaic mode observations, where large angular scale structure greater than the primary beam is imaged, the aperture errors would effectively lead to imaging errors. The dynamic range would be limited by visibility phase errors of $\Delta\varphi\sqrt{2}$ degrees in the short spacing visibilities that are recovered by the mosaicing process.

A 3% gain loss implies aperture phase errors of 10 degrees r.m.s. and this would lead to about 14 degrees r.m.s. phase errors in the visibility domain.

Summary:

- The loss in antenna power gain arising from gravity deformations may be recovered, to within 2-3% of the optimum value, by elevation dependent
    1) Axial repositioning of the SR or the feed, and
    2) Either one of
        a) A lateral displacement of the feed, or
        b) A lateral displacement of the SR, or
        c) A tilt to the SR.

- There is not much to choose between lateral displacements to the feed and tilts to the SR. At low elevations, SR off-axis displacements are marginally better than feed off-axis displacements; however, the advantage for the antenna power gain is only at the 1% level.

- The range of movement required is about ±15mm for feed displacements and ±1.5mm for SR displacements. If the compensation is made via SR rotations, a range of ±0.075 degrees rotation is required; this corresponds to tilts that move the edge of the SR over ±2 mm.

- If the compensating off-axis displacements are implemented as SR offsets, an accuracy of about ±0.05 mm is required; if the feed is repositioned, the required accuracy is relaxed to ±0.5 mm.

- The 3-mm feeds are currently on a translator; however, the translation is at an angle of 30-35 degrees to the x-axis. Feed translation could be implemented either by adding an orthogonal dimension and converting the 1D translator into a 2D translator, or by combining the existing 1D translator with fine control on the turret rotation.

- An alternate possibility is to combine the 1D feed translator with an orthogonal 1D SR translator.

- The analysis of gravity deformation in ca02 shows that the displacement vectors on the MR are not wholly confined to the x-z plane in which gravity acts. Consequently, compensation requires displacements parallel to the elevation axis (or SR tilts about the x-axis). However, most of the gain loss recovery is achieved with the axial repositioning along with purely x-component SR or feed displacement or a rotation of the SR about the y-axis. Adding the y-component displacement (or SR rotation about the x-axis) improves the gain by, additionally, only about 1%.

- These suggest that the gravity deformation compensation might be implemented as an axial repositioning of the SR, plus a 1-D translation of either the feed or SR in a direction perpendicular to the elevation axis. Alternately, an axial SR movement plus a rotation of the SR about the elevation axis might implement the compensation.

- Active axial repositioning of the SR or feed would have to be accompanied by antenna based corrections to the visibility phase. Active off-axis displacements would have to be accompanied by pointing corrections.